Electronic Supplementary Material

Graphene-like *h*-BN supported polyhedral NiS_2/NiS nanocrystals with excellent photocatalytic performance for removing rhodamine B and Cr(VI)

Wei Wang[1], Linlin Song[1], Huoli Zhang (✉)[1], Guanghui Zhang[1], Jianliang Cao (✉)[1,2]

1 College of Chemistry and Chemical Engineering, Henan Key Laboratory of Coal Green Conversion, Henan Polytechnic University, Jiaozuo 454000, China

2 State Collaborative Innovation Center of Coal Work Safety and Clean-efficiency Utilization, Henan Polytechnic University, Jiaozuo 454000, China

E-mails: zhanghuoli@hpu.edu.cn (Zhang H); caojianliang@hpu.edu.cn (Cao J)

In the work, NiS_2/NiS as a mixed crystal, the band gap energy of NiS and NiS_2 can't be separately measured. So we found new methods to prepare pure NiS nanoparticals and polyhedral NiS_2 [1,2]. Fig. S1 shows VB spectra of *h*-BN, NiS and NiS_2. XPS valence band spectra were further measured to estimate the valence band (VB) positions of *h*-BN, NiS and NiS_2. The VB of *h*-BN (3.47 eV) (Fig. S1a), NiS (0.77 eV) (Fig. S1b) and NiS_2 (1.24 eV) (Fig. S1c) is basically in line with that in schematic mechanism (*h*-BN (3.51 eV), NiS (0.53 eV) and NiS_2 (1.19 eV)). In addition, the flat-band potential were investigated by the Mott-Schottky curve (Fig. S2). The plot slope of NiS, NiS_2/NiS and 7 wt.% *h*-BN/NiS_2/NiS was negative, while the plot slope of NiS_2 and *h*-BN was positive, indicating that the former is p-type semiconductor and the latter is n-type material [3,4]. Furthermore, as revealed, the flat-band potential of the *h*-BN (n-type material) [5] and other samples are -0.82 eV (*h*-BN, vs AgCl) (Fig. S2a), 0.84 eV (NiS, vs AgCl) (Fig. S2b), -0.84 eV (NiS_2, vs

AgCl) (Fig. S2c), 1.01 eV (NiS_2/NiS, vs AgCl) (Fig. S2d), and 1.04 eV (7 wt.% *h*-BN/NiS_2/NiS, vs AgCl) (Fig. S2e), respectively. Corrected by the AgCl (vs 0.197 eV), the Fermi level of the samples could be calculated to be -0.623 eV (*h*-BN, vs NHE), -0.643 eV (NiS, vs NHE), -0.643 eV (NiS_2, vs NHE), -0.804 eV (NiS_2/NiS, vs NHE), and -0.843 eV (7 wt.% *h*-BN/NiS_2/NiS, vs NHE), respectively. As revealed, the E_f-NiS = E_f-NiS_2 < E_f-NiS_2/NiS < E_f-*h*-BN < E_f-7 wt.% *h*-BN/NiS_2/NiS, which indicates that the photon-generated electron would transfer along the route of the NiS, NiS_2 to *h*-BN, that process could promote the separation, transferring and diffusion of the photon-generated carriers efficiently, and the result is in line with XPS.

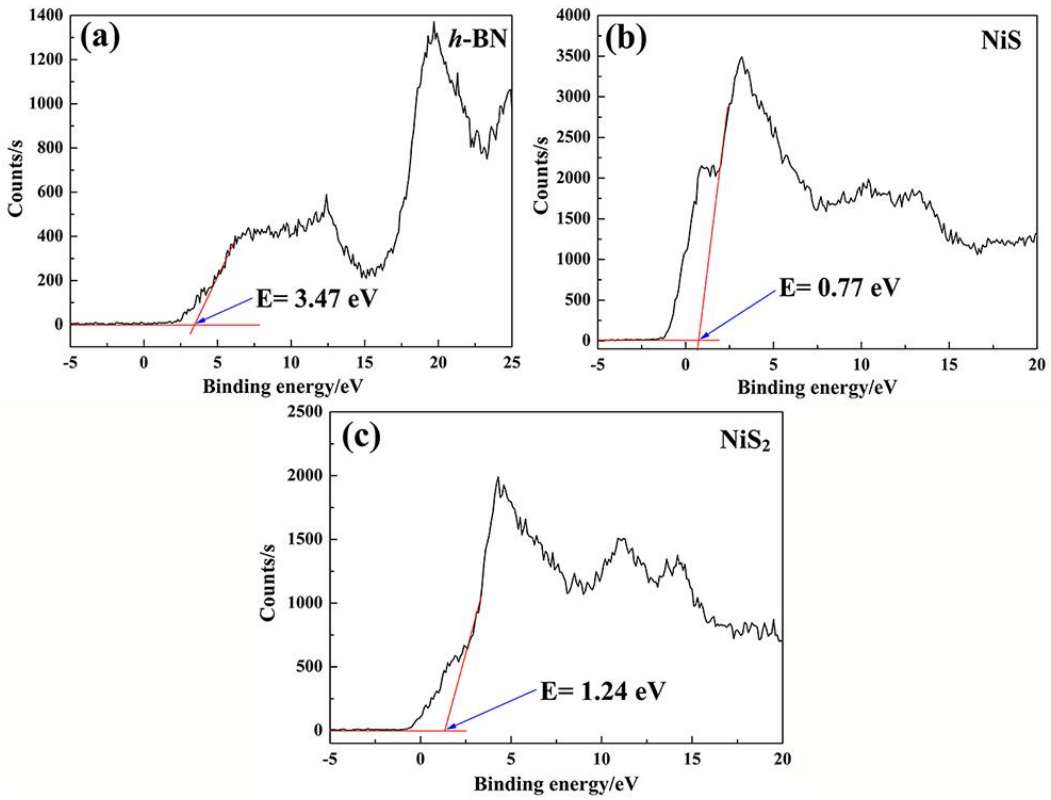

Fig. S1 VB XPS spectra of (a) *h*-BN; (b) NiS; (c) NiS_2.

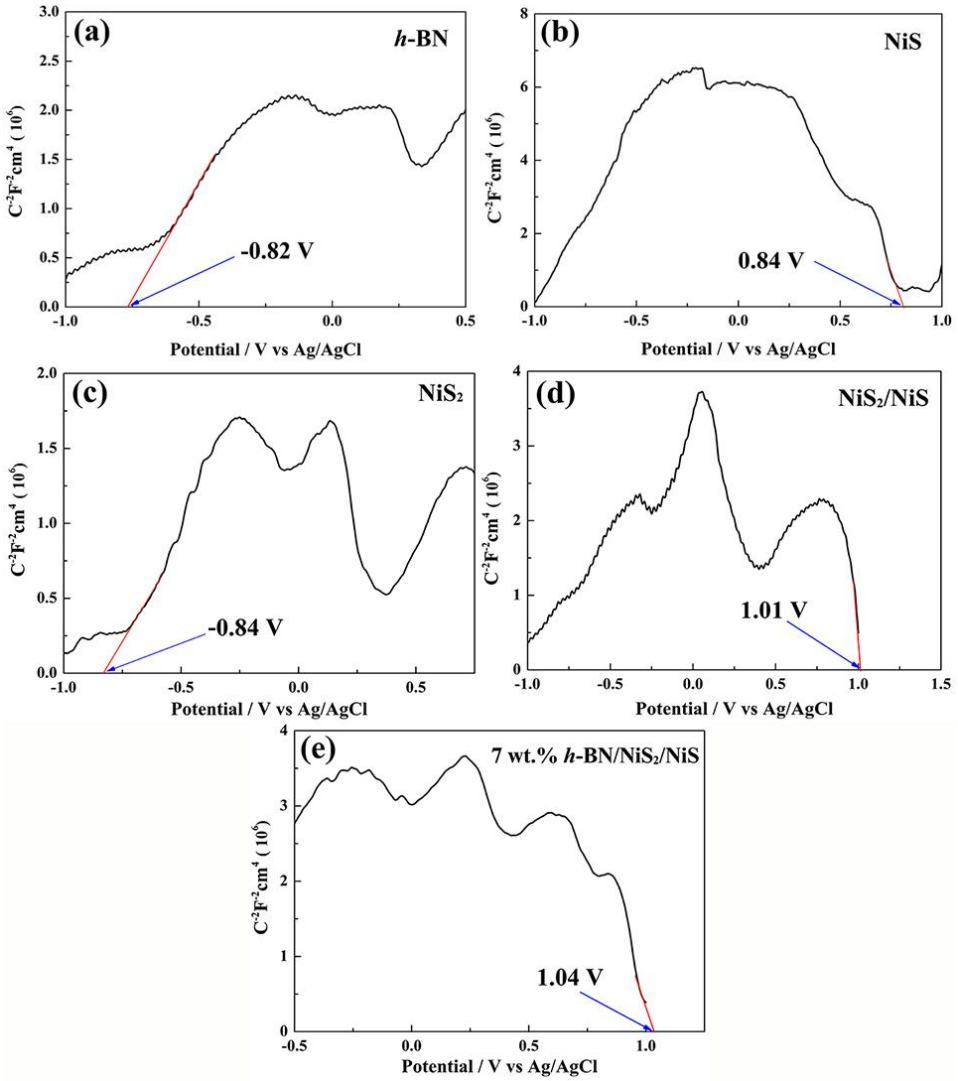

Fig. S2 The Mott-schottky plots of the different samples.

References

1. Liang Y, Yang Y, Xu K, Yu T, Yang Q, Shi P, Yuan C. Crystal facets engineering and rGO hybridizing for synergistic enhancement of photocatalytic activity of nickel disulfide. Journal of Hazardous Materials, 2020, 384: 121402

2. Li L, Wu J, Liu B, Liu X, Li C, Gong Y, Huang Y, Pan L. NiS sheets modified CdS/reduced graphene oxide composite for efficient visible light photocatalytic hydrogen evolution. Catalysis Today, 2018, 315: 110-116

3. Sartale S D, Lokhande C D. Preparation and characterization of nickel sulphide thin films using successive ionic layer adsorption and reaction (SILAR) method. Materials Chemistry and Physics, 2001, 72: 101-104
4. Jourshabani M, Shariatinia Z, Achari G, Langford C H, Badiei A. Facile synthesis of NiS_2 nanoparticles ingrained in a sulfur-doped carbon nitride framework with enhanced visible light photocatalytic activity: two functional roles of thiourea. Journal of Materials Chemistry A, 2018, 6 (27): 13448-13466
5. Acharya L, Nayak S, Pattnaik S P, Acharya R, Parida K. Resurrection of boron nitride in p-n type-II boron nitride/B-doped-g-C_3N_4 nanocomposite during solid-state Z-scheme charge transfer path for the degradation of tetracycline hydrochloride. Journal of Colloid and Interface Science, 2020, 566: 211-223